Reaction and Free Radical Kinetics of Prostaglandin H Synthase with Manganese Protoporphyrin IX as the Prosthetic Group[†,‡]

Richard J. Kulmacz,*[,§] Graham Palmer,[‖] Chunhong Wei,[§] and Ah-Lim Tsai[§]

Division of Hematology, Department of Internal Medicine, University of Texas Health Science Center at Houston, Houston, Texas 77030, and Department of Biochemistry and Cell Biology, Rice University, Houston, Texas 77251

Received November 28, 1993; Revised Manuscript Received February 15, 1994[⊕]

ABSTRACT: Prostaglandin H synthase (PGHS) is a hemoprotein with both cyclooxygenase and peroxidase activities. Several aspects of the peroxidase and cyclooxygenase activities and the formation of substrate-induced free radical species were characterized with ovine seminal vesicle PGHS reconstituted with manganese protoporphyrin IX (Mn–PGHS) for comparison with the enzyme-containing heme (Fe–PGHS). Compared to Fe–PGHS, the K_m of Mn–PGHS peroxidase for ethyl hydroperoxide was much higher, but that for 15-hydroperoxyeicosatetraenoic acid (15-HPETE) was little changed. The Mn–PGHS peroxidase V_{max} value with 15-HPETE was about 4% that with Fe–PGHS. Mn–PGHS oxidized 0.95 ± 0.05 and Fe–PGHS oxidized 2.06 ± 0.09 mol of TMPD/mol of 15-HPETE. Reaction of 15-HPETE with Mn–PGHS resulted in approximately equal proportions of two lipid products: 15-hydroxyeicosatetraenoic acid (15-HETE) and a compound identified as 15-ketoeicosatetraenoic acid. Fe–PGHS produced only 15-HETE. Thus, 15-HETE can serve as an efficient two-electron reductant of oxidized Mn–PGHS intermediates. The rate of accumulation of oxidized Mn–PGHS intermediate was dependent on the substrate, decreasing in the following order: 15-HPETE > 11,14-eicosadienoate > arachidonate > EtOOH. The cyclooxygenase specific activity increased in a saturable fashion as the concentration of Mn–PGHS was increased, reaching a value higher than that for Fe–PGHS. Computer simulations of the reaction kinetics indicated that this dependence on the Mn–PGHS level was a consequence of the low rate of formation of oxidized peroxidase intermediate. Incubation of Mn–PGHS with either 15-HPETE or arachidonate resulted in the rapid production of a free radical species. The initial accumulation of radical coincided with the synthesis of PGG_2 and PGH_2, indicating that the radical was kinetically competent to participate in cyclooxygenase catalysis. Reaction with tetranitromethane, a reagent that selectively nitrates tyrosyl residues, destroyed the cyclooxygenase activity of Mn–PGHS, resulting in a much narrower free radical EPR signal. These effects indicate that tyrosine residues are essential for cyclooxygenase activity and that they influence the radical structure in Mn–PGHS.

Prostaglandin H synthase (PGHS[1]), with heme as the prosthetic group, catalyzes both cyclooxygenase and peroxidase reactions. The two reactions have been proposed to be linked mechanistically, with a tyrosyl radical generated from a peroxidase cycle intermediate acting as the key oxidant in the cyclooxygenase reaction (Kulmacz et al., 1985; Kulmacz, 1986; Karthein et al., 1988). Replacement of the heme with manganese protoporphyrin IX results in the retention of a considerable part of the cyclooxygenase activity and the loss of about 99% of the peroxidase activity (Ogino et al., 1978; Odenwaller et al., 1992; Strieder et al., 1992). These selective perturbations have made the MnPPIX-substituted enzyme (Mn–PGHS) an important experimental subject for elucidation of the details of the cyclooxygenase and peroxidase reaction mechanisms, particularly for testing the proposed role of oxidized peroxidase intermediates and hydroperoxide-induced radicals in cyclooxygenase catalysis.

To better understand the effects of the change in metalloporphyrin on catalysis by the synthase, we have compared the peroxidase and cyclooxygenase kinetics of Mn–PGHS and Fe–PGHS with a variety of substrates. The results indicate that besides exhibiting a decreased peroxidase activity, Mn–PGHS has a higher specificity for fatty acid hydroperoxides, and only Mn–PGHS utilizes some hydroxy fatty acid as a reducing cosubstrate. The autocatalytic nature of the cyclooxygenase reaction was found to be much more manifest in Mn–PGHS than in Fe–PGHS. Kinetic modeling based on the proposed mechanism showed that the difference in this central aspect of cyclooxygenase activity is actually an expected consequence of the observed lower peroxidase activity in Mn–PGHS. In spite of the specific differences between Mn–PGHS and Fe–PGHS, the kinetic behavior of Mn–PGHS appears to be consistent with the general reaction mechanism proposed for Fe–PGHS.

Lassmann et al. (1991) reported that the incubation of Mn–PGHS with arachidonate resulted in the generation of a significant level of free radical, but only after oxygenation of

[†] This work was supported in part by United States Public Health Service Grants GM 30509 (to R.J.K.), GM 21337 (to G.P.), and GM 44911 (to A.-L.T.) and Welch Foundation Grant C636 (to G.P.).

[‡] A preliminary report of a portion of this work was presented at the 8th International Conference on Prostaglandins and Related Lipids in Montreal, Canada, July, 1992; a preliminary account of this report appeared in *J. Lipid Mediators 6*, 145–154 (1993).

* Author to whom correspondence should be addressed.

[§] University of Texas Health Science Center at Houston.

[‖] Rice University.

[⊕] Abstract published in *Advance ACS Abstracts*, April 1, 1994.

[1] Abbreviations: PGHS, prostaglandin H synthase; FePPIX and MnPPIX, iron and manganese protoporphyrins IX, respectively; Fe–PGHS and Mn–PGHS, prostaglandin H synthase reconstituted with FePPIX and MnPPIX, respectively; ROOH, hydroperoxide; EtOOH, ethyl hydrogen peroxide; 15-HPETE, 15-hydroperoxyeicosa-5,8,11,13-tetraenoic acid; 15-HETE, 15-hydroxyeicosa-5,8,11,13-tetraenoic acid; 20:2, 11,14-eicosadienoic acid; 11-HPEDE, 11-hydroperoxyeicosa-12,14-dienoic acid; 11-HEDE, 11-hydroxyeicosa-12,14-dienoic acid; TNM, tetranitromethane; TMPD, *N,N,N′,N′*-tetramethyl-*p*-phenylenediamine; EPR, electron paramagnetic resonance; HPLC, high-pressure liquid chromatography.

0006-2960/94/0433-5428$04.50/0

the fatty acid was complete. However, as we have shown subsequently (Tsai et al., 1992), the reaction conditions used by Lassmann et al. (1991) result in atypical cyclooxygenase characteristics, including self-inactivation so extraordinarily rapid that it limits fatty acid oxygenation to as little as 1 mol/mol of synthase. As a consequence of this rapid and complete self-inactivation, EPR signals from a diminishing fraction of native synthase would be obscured by other signals from the rapidly increasing fraction of inactivated enzyme. This expectation is supported by the recent report of DeGray et al. (1992) that the EPR spectrum observed early in the reaction of Fe–PGHS with arachidonate was dominated by a wide doublet characteristic of native enzyme (Tsai et al., 1992), whereas the major contribution to the spectrum later in the reaction was from a narrow singlet similar to that found in synthase inactivated with indomethacin or aspirin (Kulmacz et al., 1990, 1991).

These complications in the interpretation of the earlier study (Lassmann et al., 1991) necessitate a reexamination of the temporal relationship between radical generation and cyclooxygenase catalysis by Mn–PGHS under conditions restricting enzyme inactivation. We have found that decreasing the arachidonate concentration to approximately that of the enzyme minimizes self-inactivation and results in EPR signals characteristic of the native Fe–PGHS (Tsai et al., 1992); we have used such conditions with Mn–PGHS, so that any radicals observed can reasonably be attributed to normal cyclooxygenase function. The present results indicate that Mn–PGHS can generate a free radical that is kinetically competent for participation in cyclooxygenase catalysis.

MATERIALS AND METHODS

Hydrogen peroxide, TMPD, TNM, and FePPIX were from Sigma Chemical Co. (St. Louis, MO). MnPPIX was from Porphyrin Products (Logan, UT). Arachidonic acid and 11,14-eicosadienoic acid were from NuChek Preps (Elysian, MN). [^{14}C]Arachidonic acid was from Amersham (Arlington, IL). EtOOH was purchased as a 5% solution from Polysciences Inc. (Warrington, PA).

15-HPETE was prepared using [1-^{14}C]arachidonic acid (Amersham Corp.) and soybean lipoxygenase as described by Graff et al. (1990) and purified by chromatography on silica. The purity of 15-HPETE was assessed by chromatography (Graff, 1982), and the concentration was determined either from the radioactivity or from spectrophotometry using excess Fe–PGHS and TMPD (Kulmacz et al., 1990).

PGH synthase was purified to electrophoretic homogeneity from ram seminal vesicles (Kulmacz & Lands, 1987). The enzyme concentration was determined by a modification of the Lowry method (Peterson, 1983) or from the absorbance at 279 nm using an extinction coefficient of 116 (mM subunit)$^{-1}$ cm^{-1}. Synthase preparations were treated with DEAE-cellulose (Kulmacz et al., 1987) in the presence of 5 mM glutathione to remove residual heme. The interaction of the synthase with MnPPIX appeared weaker than that with FePPIX, because MnPPIX was more easily removed from the synthase by treatment with DEAE-cellulose (data not shown). Consequently, removal of excess MnPPIX for spectroscopic experiments was accomplished by gel filtration on a Bio-Rad 10DG column. Holoenzyme solutions for most enzymological assays were prepared by incubating apoenzyme with either FePPIX (1 mol/mol of subunit) or MnPPIX (2 mol/mol of subunit) for about 30 min at room temperature; these stoichiometries are above those required for maximal activity in standard assays (Kulmacz & Lands, 1984), avoiding the need to add metalloporphyrin to the reaction buffer.

Cyclooxygenase activity was assayed using a polarographic oxygen electrode (Kulmacz & Lands, 1987). The standard reaction mixture included 3 mL of 0.1 M potassium phosphate (pH 7.2), 0.1 mM arachidonate, and 1 μM heme thermostated at 30 °C; the reaction was started by injection of the enzyme. The peak cyclooxygenase velocity in each reaction (V_{opt}) was calculated either graphically from the chart recorder tracing or by electronic differentiation of the digitized electrode signal (Kulmacz & Lands, 1987). In all cases, V_{opt} was reached before 10% of the arachidonate was consumed. The K_m value is below 5 μM arachidonate for both Fe–PGHS (Marshall et al., 1987) and Mn–PGHS (R. Kulmacz, unpublished observation), so that changes in fatty acid before V_{opt} was reached would have a negligible effect on cyclooxygenase velocity. One unit of cyclooxygenase gives a V_{opt} of 1 nmol of O_2/min under standard assay conditions. The synthase preparations used in this study had cyclooxygenase specific activities of 40–70 units/μg of protein.

Peroxidase activity was assayed using TMPD as the chromogenic cosubstrate and 15-HPETE or EtOOH as the substrate (Kulmacz, 1987). The standard reaction mixture included 2 mL of 0.1 M Tris (pH 8.0) and 84 μM TMPD stirred continuously at 25 °C. The reaction was initiated by injection of the hydroperoxide. The increase in absorbance at 611 nm due to oxidized TMPD was measured with a Shimadzu Model 2101 spectrophotometer. The spectrum of oxidized TMPD formed during the reaction of 15-HPETE with Mn–PGHS was found to be identical with that of oxidized TMPD formed by Fe–PGHS. The peroxidase velocity was calculated from the first derivative of the absorbance extrapolated to t_0 (to compensate for self-inactivation), using an extinction coefficient of 13.5 (mM $TMPD_{ox}$)$^{-1}$ cm^{-1} (Kulmacz, 1987). The stoichiometry between TMPD oxidation and hydroperoxide reduction was taken to be 2.0 for Fe–PGHS (Reed et al., 1985; Kulmacz, 1986).

For evaluation of the stoichiometry between 15-HPETE consumption and TMPD oxidation, Mn–PGHS or Fe–PGHS was incubated in a cuvette containing 2.0 mL of 0.1 M Tris (pH 8.0) and 10–260 μM TMPD. The reaction was started by the addition of 15-HPETE (12.4 μM final) in 15 μL of ethanol. This level of solvent had no effect on the reaction. The oxidation of TMPD was monitored continuously from absorbance changes at 611 nm (Kulmacz, 1987). After the reaction subsided (45–90 s), the surviving hydroperoxide was quantitated from the additional TMPD oxidation that occurred upon the injection of excess Fe–PGHS, using a stoichiometry of 2.0 mol of $TMPD_{ox}$/mol of 15-HPETE (Reed et al., 1985; Kulmacz, 1986).

To study the relationship between cyclooxygenase activity and radical formation during the reaction of Mn–PGHS with arachidonate, the enzyme and fatty acid solutions were mixed within a few milliseconds with a homemade, hand-driven, two-syringe, equal-mixing device connected to a four-jet tangential mixer (G. Palmer, unpublished results). The syringes, mixer, and connecting tubing were immersed in an ice bath, and the experiment was conducted in a cold room at 4 °C. Details have been described previously (Tsai et al., 1992). For EPR observations, the reaction mixture was collected in an EPR tube on ice and quenched after the desired delay by plunging the tube into a dry ice/acetone bath; samples froze within 1 s. EPR spectra were recorded at liquid nitrogen temperatures, and radical concentrations were determined by reference to a copper standard, as described previously (Kulmacz et al., 1990). A buffer blank was used to correct for background signals. Parallel reactions with the same apparatus and [^{14}C]-

Table 1: Heme Content and Enzymatic Activity in PGHS Apoenzyme

	heme/subunit	peroxidase velocity[c] ($TMPD_{ox}$/s/subunit) EtOOH	15-HPETE
apoenzyme	0.03[a]	0.5 (0.1%)	0.4 (0.1%)
apoenzyme + FePPIX	1.0[b]	552 (100%)	465 (100%)

[a] Calculated from A_{411} using an extinction coefficient of 165 mM^{-1} cm^{-1}. [b] Added FePPIX. [c] Determined from the increase in A_{611} after the addition of 2.0 mM EtOOH or 16.8 μM 15-HPETE to reaction mixtures containing PGHS and 84 μM TMPD at 25 °C.

arachidonate were used to quantitate cyclooxygenase catalysis as described previously (Tsai et al., 1992). For this, the reaction mixture was collected in a glass test tube on ice and quenched after the desired delay by vigorous addition of ice-cold acidified organic solvent and vortexing. The conversion of arachidonate to PGG_2 and PGH_2 was quantitated after analysis of the lipid products by thin-layer chromatography.

RESULTS

Residual Heme in Apoenzyme Preparations. The ability of the DEAE-cellulose treatment procedure to remove endogenous heme quantitatively from purified ram seminal vesicle PGHS was examined by assay of the peroxidase activity of apoenzyme before and after reconstitution with fresh metalloporphyrin. The peroxidase activity with either EtOOH or 15-HPETE as substrate was found to increase by over 1000-fold upon reconstitution with fresh heme (Table 1), indicating that the level of contamination of the apoenzyme with functional heme was about 0.1%. In contrast, the residual heme level estimated from the Soret absorbance was 0.03 mol/mol of apoenzyme subunit (Table 1). It is thus clear that very little of the residual Soret absorbance in the apoenzyme was due to functional heme and that only a negligible part of the enzymatic activity of Mn–PGHS can be ascribed to contaminating Fe–PGHS.

Comparison of Peroxidase K_m and V_{max} of Mn–PGHS and Fe–PGHS. Two different hydroperoxide substrates were used for the comparison of peroxidase activity: EtOOH, a small water-soluble hydroperoxide, and 15-HPETE, a fatty acid hydroperoxide. The peroxidase velocity with each hydroperoxide was a linear function of added enzyme for both Fe–PGHS and Mn–PGHS (data not shown). The dependence of peroxidase velocity on substrate concentration was examined, with the concentration of Fe–PGHS fixed at 11.1 nM subunit and that of Mn–PGHS at 145 nM subunit. With EtOOH as substrate, Fe–PGHS exhibited conventional Michaelis–Menten kinetics, and a nonlinear least-squares procedure was used to estimate a K_m of 0.46 ± 0.04 mM EtOOH and a V_{max} of 410 ± 18 mol of EtOOH/s/mol of subunit. In contrast, the Mn–PGHS peroxidase activity showed no sign of saturation even at 9.8 mM EtOOH, the higest concentration examined. Thus, the K_m of Mn–PGHS for EtOOH was more than 10 mM. Although a value for V_{max} could not be obtained, the peroxidase velocity at the highest level of EtOOH was about 3 mol of EtOOH/s/mol of subunit for Mn–PGHS, which is about 0.7% of the V_{max} value found with Fe–PGHS.

With 15-HPETE as substrate, saturation kinetics were observed for both Fe–PGHS and Mn–PGHS. For Fe–PGHS, the estimated K_m was 5.1 ± 1.2 μM and the estimated V_{max} was 290 ± 36 mol of 15-HPETE/s/mol of subunit. The corresponding estimates for Mn–PGHS were 11.3 ± 1.7 μM 15-HPETE for K_m and 11.0 ± 0.7 mol of 15-HPETE/s/mol of subunit for V_{max}. Thus, the affinities of Mn–PGHS and Fe–PGHS for the lipid hydroperoxide were comparable. This clearly was not the case with the water-soluble hydroperoxide, indicating that the substrate selectivity is much higher with Mn–PGHS than with Fe–PGHS. Comparison of the V_{max} values with 15-HPETE as substrate indicates that the turnover number for Mn–PGHS was about 4% of that with Fe–PGHS.

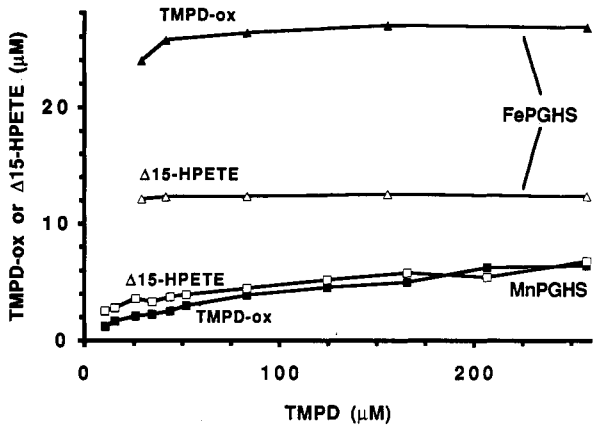

FIGURE 1: TMPD oxidation and consumption of 15-HPETE by Mn–PGHS and Fe–PGHS. A fixed level (50 nM subunit) of Mn–PGHS (■, □) or Fe–PGHS (▲, △) was incubated with the indicated concentrations of TMPD in 0.1 M Tris (pH 8.0), thermostated at 15 °C before the addition of 15-HPETE (final concentration, 12.4 μM). After the reaction subsided (45–90 s), the levels of TMPD oxidation (■, ▲) and hydroperoxide consumption (□, △) were determined as described in Materials and Methods.

Stoichiometry of TMPD Oxidation and Hydroperoxide Consumption. The relationship between hydroperoxide consumption and cosubstrate oxidation was examined by incubating the same fixed concentration of Mn–PGHS or Fe–PGHS with a fixed concentration of 15-HPETE in the presence of a variable level of TMPD. The oxidation of TMPD was determined from the absorbance at 611 nm, and the 15-HPETE consumption was determined from the difference between the initial hydroperoxide level and that surviving at the end of the incubation. The results (Figure 1) indicate that essentially all of the hydroperoxide was consumed by Fe–PGHS in the initial reaction at all levels of TMPD. TMPD oxidation was twice the 15-HPETE consumption (ratio of 2.13 ± 0.03 for the four highest levels of TMPD), confirming earlier studies (Reed et al., 1985; Kulmacz, 1986).

With Mn–PGHS the extent of the initial reaction was limited by enzyme inactivation at all TMPD concentrations. The continued availability of hydroperoxide and cosubstrate after the reaction with Mn–PGHS ceased was confirmed by the observation of additional TMPD oxidation upon addition of Fe–PGHS. Mn–PGHS thus decomposed less 15-HPETE than did Fe–PGHS at all TMPD levels examined, indicating that the peroxidase self-inactivation of Mn–PGHS was more efficient than that of Fe–PGHS. Surprisingly, TMPD oxidation with Mn–PGHS was almost equal to 15-HPETE consumption at cosubstrate levels above 50 μM (ratio of 0.96 ± 0.11). This stoichiometry of cosubstrate oxidation/hydroperoxide decomposition is only one-half that observed with Fe–PGHS.

The stoichiometry between hydroperoxide reduction and TMPD oxidation was also examined with two hydroperoxides generated in situ by the cyclooxygenase activity of the synthase: 11-HPEDE (from 11,14-eicosadienoic acid; Hemler et al., 1978a) and PGG_2 (from arachidonic acid). In these reactions, excess Mn–PGHS or Fe–PGHS and excess TMPD were used to ensure that all of the fatty acid was consumed

Table 2: Stoichiometry of TMPD Oxidation and Hydroperoxide Reduction with Mn–PGHS and Fe–PGHS

hydroperoxide	reaction stoichiometry[a] (mol of TMPD oxidized/ mol of ROOH reduced)	
	Mn–PGHS	Fe–PGHS
PGG_2 (in situ from arachidonate)	1.71 ± 0.07 (n = 3)	2.24 ± 0.04 (n = 5)
11-HPEDE (in situ from 11,14-eicosadienoate)	1.16 ± 0.12 (n = 6)	2.27 ± 0.06 (n = 4)
15-HPETE	0.95 ± 0.05 (n = 3) 0.96 ± 0.11 (n = 4)[b]	2.06 ± 0.09 (n = 7)

[a] Excess Mn–PGHS or Fe–PGHS was incubated in 2 mL of 0.1 M Tris (pH 8.0), with at least 84 μM TMPD. Reaction was initiated by the addition of arachidonate, 11,14-eicosadienoate, or 15-HPETE at a final concentration of 1.3–12.1 μM. Oxidation of TMPD was calculated from the final increase in A_{611} (corrected for nonenzymatic oxidation) using an extinction coefficient of 13.5 mM^{-1} cm^{-1}. The values shown represent the mean ● standard deviation for the indicated number of replicates. [b] Reaction was limited by the level of Mn–PGHS (taken from data in Figure 1 for the four highest levels of TMPD).

and that the amount of hydroperoxide was the factor limiting the oxidation of TMPD. Similar reactions were performed wtih 15-HPETE and excess enzyme. Fe–PGHS exhibited a stoichiometry of about 2 TMPD oxidized/hydroperoxide consumed for each hydroperoxide (Table 2). In contrast, with Mn–PGHS the stoichiometry was about 1 for 11-HPEDE and 15-HPETE and approached 2 only for PGG_2. Thus, the oxidation stoichiometry observed with Mn–PGHS appeared to depend on the structure of the hydroperoxide, and not whether the hydroperoxide was generated endogenously by the cyclooxygenase. The stoichiometry for Mn–PGHS with 15-HPETE was essentially the same when the reaction was limited by the enzyme concentration rather than by the substrate concentration.

Analysis of Lipid Reaction Products. The unexpectedly low stoichiometry of TMPD oxidation with Mn–PGHS and some hydroperoxides suggested an alternate source of reducing equivalents, perhaps from the lipid substrate. To characterize reaction products from lipid hydroperoxide, a fixed amount of [^{14}C]-15-HPETE was incubated with increasing amounts of Mn–PGHS in the presence of excess TMPD, and the lipid products were analyzed by thin-layer chromatography. For comparison, parallel reactions were run with Fe–PGHS. From the autoradiogram in Figure 2, it is evident that Fe–PGHS formed a single product (R_f 0.17) that was slightly more polar than 15-HPETE (R_f 0.23), consistent with the expected alcohol, 15-HETE (Eling et al., 1985). As the concentration of Fe–PGHS was increased, there was a progressive decrease in the intensity of the 15-HPETE band and a corresponding increase in the 15-HETE band, indicating that the enzyme was the limiting factor.

In contrast, Mn–PGHS formed two distinct products: one that comigrated with 15-HETE and one (R_f 0.28) that was less polar than the starting material. This less polar band gave a positive reaction with 2,4-dinitrophenylhydrazine (Vioque & Holman, 1962), demonstrating the presence of a carbonyl function. The intensities of the two product bands from 15-HPETE increased in parallel with the level of Mn–PGHS (Figure 2). The ratio of the intensity of the R_f 0.28 band to that of 15-HETE (determined by densitometry) averaged 0.82 ± 0.05 for the five reactions with the highest Mn–PGHS levels. This suggests that Mn–PGHS formed the two products in roughly equal proportions.

The products from reactions of 15-HPETE with Mn–PGHS and Fe–PGHS were also analyzed by HPLC. With Fe–PGHS, only one peak was seen (labeled B in Figure 3); it had an absorbance spectrum with a prominent peak at 232 nm (Figure 3 inset, spectrum 2), as expected for the conjugated diene chromophore in 15-HETE. Two peaks were observed in the HPLC chromatogram of the Mn–PGHS products (Figure 3). Peak B eluted at about the same time as the 15-HETE peak produced by Fe–PGHS and had essentially the same absorbance spectrum (Figure 3 inset, spectrum 3). Peak A eluted earlier than 15-HETE, reflecting lower polarity. Pooled fractions of peak A had an absorbance maximum at 278 nm (Figure 3 inset, spectrum 1), consistent with the presence of a keto diene chromophore (Vioque & Holman, 1962). Judging from its decreased polarity relative to 15-HETE on chromatography, its positive reaction with 2,4-dinitrophenylhydrazine, and its UV spectrum, the second Mn–PGHS product is probably 15-ketoeicosa-5,8,11,13-tetraenoic acid.

The lipid products extracted from reaction of 20:2 with Mn–PGHS in the presence of excess TMPD had a pronounced absorbance peak near 275 nm, much like the reaction products from 15-HPETE (data not shown). HPLC analysis of the Mn–PGHS products with 20:2 revealed a single major peak of 275 nm absorbance, which eluted after the keto diene produced from 15-HPETE (Figure 4). The lipid extract from a parallel reaction of Fe–PGHS with 20:2 lacked significant absorbance at 275 nm and, when analyzed by HPLC, displayed only a trace of the peak seen with Mn–PGHS (Figure 4).

Spectroscopic Changes during the Reaction of Mn–PGHS with Substrate. The absorbance spectrum of Mn–PGHS was monitored during reaction of the enzyme with two hydroperoxides (15-HPETE and EtOOH) and two fatty acid substrates for the cyclooxygenase (arachidonate and 11,14-eicosadienoate). These substrates were chosen because EtOOH and 15-HPETE exhibited very different kinetics of TMPD oxidation, and the hydroperoxides generated from the two fatty acids were found to have very different stoichiometries of TMPD oxidation (Table 2). Resting Mn–PGHS exhibited absorbance maxima at 374, 471, and 556 nm, essentially as reported by Strieder et al. (1992) and Odenwaller et al. (1992). Reaction of Mn–PGHS with EtOOH, 15-HPETE, arachidonate, or 11,14-eicosadienoate resulted in qualitatively the same absorbance changes as those reported by Strieder et al. (1992) and Odenwaller et al. (1992), with decreases at 374 and 471 nm and the appearance of a new peak at 418 nm. However, different reaction kinetics were observed with individual substrates, as judged from the absorbance changes at 418 nm (Figure 5). The rate of the initial absorbance increase at 418 nm was highest for 15-HPETE and decreased in the following order: 11,14-eicosadienoate > arachidonate > EtOOH. The absorbance changes were reversed with further incubation, indicating that the oxidized form of Mn–PGHS was not stable. The isosbestic points apparent in this second phase of the reaction were the same as those seen immediately after the addition of substrate (data not shown), indicating that a simple reversal of the initial transition was occurring. The decline in the concentration of the oxidized species was fastest for 15-HPETE and 11,14-eicosadienoate, much slower for arachidonate, and very much slower for EtOOH (Figure 5).

Pretreatment of Mn–PGHS with indomethacin, a cyclooxygenase inhibitor, greatly decreased the accumulation of oxidized intermediate during reaction with 15-HPETE (Figure 5). The effect of indomethacin on the steady-state peroxidase activity of Mn–PGHS was also examined, using 16 μM 15-HPETE as substrate under standard conditions

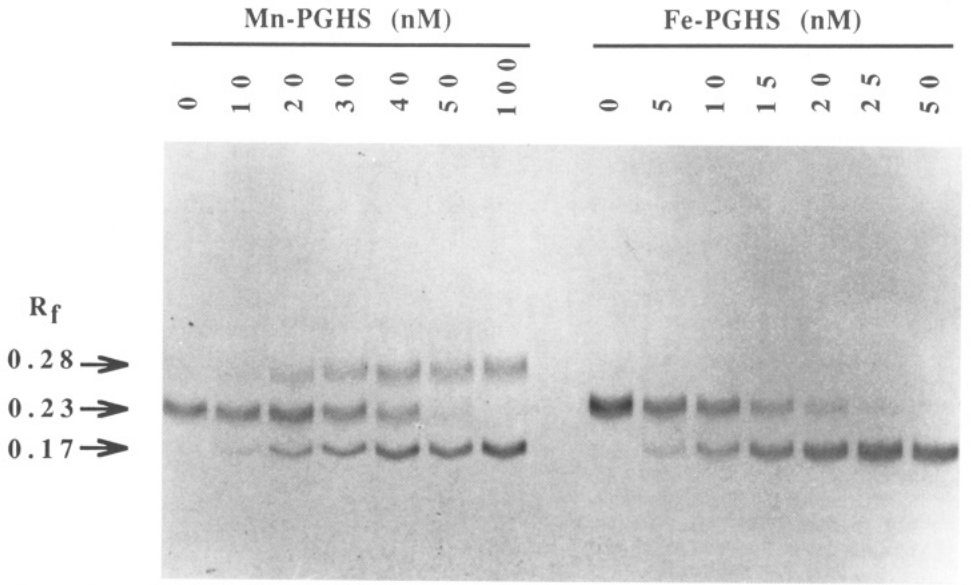

FIGURE 2: Thin-layer chromatography of 15-HPETE reaction products with Mn–PGHS and Fe–PGHS. The indicated concentrations of Mn–PGHS and Fe–PGHS were mixed with 2.0 mL of 0.1 M Tris (pH 8.0) containing 105 μM TMPD in a stirred spectrophotometer cuvette thermostated at 21 °C. Reaction was begun by the addition of [^{14}C]-15-HPETE (2.0 μCi/μmol) in 15 μL of ethanol to give a final concentration of 12.7 μM, and the oxidation of TMPD was monitored from the increase in absorbance at 611 nm. After 120 s, when TMPD oxidation was essentially complete, the lipid products were extracted (Miyamoto et al., 1976) by the addition of 3 vol of ice-cold diethyl ether/methanol/1 M citric acid (30:4:1). The extracts were dried with anhydrous sodium sulfate, and the solvent was evaporated under a stream of nitrogen. The residue was dissolved in a small volume of ethyl acetate/hexane (1:1) and applied to the preabsorbent zone of a Whatman LK6D silica gel plate. The plate was developed at room temperature with diethyl ether/hexane/glacial acetic acid (55:45:0.1) to 14.5 cm above the origin. Bands were visualized by autoradiography.

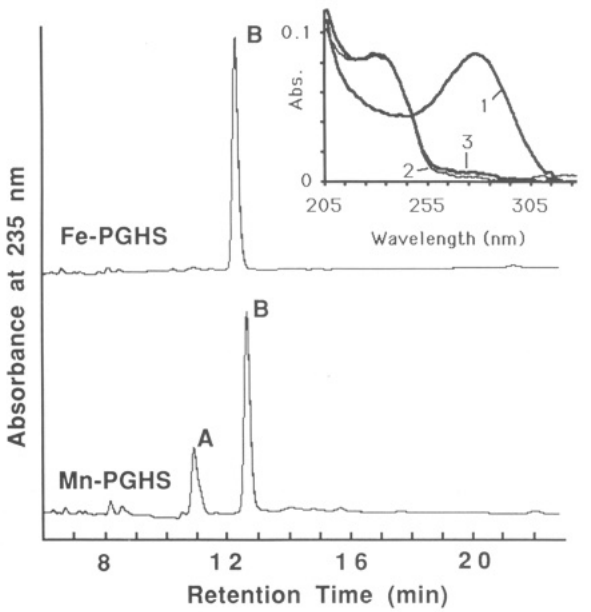

FIGURE 3: HPLC analysis of 15-HPETE reaction products with Mn–PGHS and Fe–PGHS. 15-HPETE (15–36 μM) was added to 3 mL of 0.1 M Tris (pH 8.0) containing 105 μM TMPD in a stirred spectrophotometer cuvette at room temperature. Excess Mn–PGHS (170 nM subunit) or Fe–PGHS (140 nM subunit) was then added, and the absorbance at 611 nm was monitored. After the reaction had subsided, reaction products were extracted as described in the legend to Figure 2. Aliquots of the reaction products were injected onto a silica column (Rainin silica MV, 4.6 × 250 mm) eluted at 1 mL/min with hexane/isopropyl alcohol/glacial acetic acid (990:10:1), with monitoring at 235 nm. Inset: Absorbance spectra of concentrated HPLC fractions containing Mn–PGHS peak A (1), Mn–PGHS peak B (2), or Fe–PGHS peak B (3).

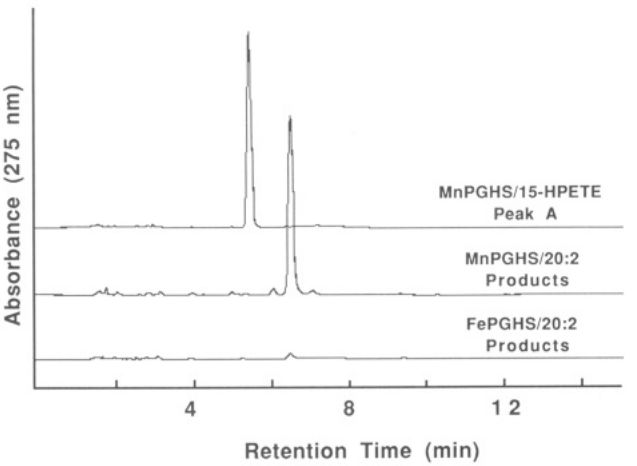

FIGURE 4: HPLC analysis of 20:2 reaction products with Mn–PGHS and Fe–PGHS. Mn–PGHS (300 nM subunit) or Fe–PGHS (140 nM subunit) was added to 2 mL of 0.1 M potassium phosphate (pH 7.2) containing 105 μM TMPD in a stirred spectrophotometer cuvette at 25 °C. Reaction was initiated by injection of 20:2 (5 mM in 0.1 M Tris-HCl, pH 8.5) to a final concentration of 40 μM. After 5 min, TMPD oxidation was quantitated from the increase in absorbance at 611 nm, and the lipid products were extracted as described in the legend to Figure 2. The extracts were analyzed as described in the legend to Figure 3, except that the flow rate was 2 mL/min and the eluate was monitored at 275 nm. Peak heights for the Mn–PGHS and Fe–PGHS products have been normalized to the amount of hydroperoxide produced, assuming stoichiometries of 2 mol of TMPD oxidized/mol of hydroperoxide for Fe–PGHS and 1 mol of TMPD oxidized/mol of hydroperoxide for Mn–PGHS (Table 2). Peak A fractions from the reaction of Mn–PGHS with 15-HPETE (Figure 3) were chromatographed for comparison.

(Materials and Methods). The control Mn–PGHS preparation had a peroxidase activity of 11.2 mol of 15-HPETE/s/mol of subunit. After preincubation with 1 equiv of indomethacin for 30 min on ice, the same preparation had only 67% of the control activity. For comparison, indomethacin treatment inhibited the Mn–PGHS cyclooxygenase activity to about 6% of the control value (data not shown), a decrease comparable to that found with Fe–PGHS (Kulmacz & Lands, 1985b).

Comparison of the Cyclooxygenase Kinetics of Mn–PGHS and Fe–PGHS. Preliminary observations suggested that

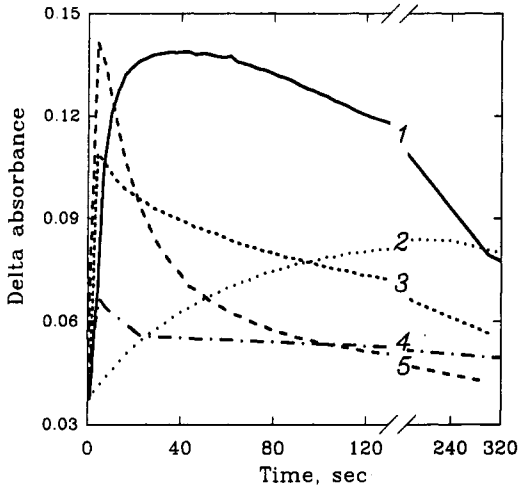

FIGURE 5: Kinetics of absorbance changes at 418 nm during reaction of Mn–PGHS with substrates. Mn–PGHS (5 μM subunit) was reacted with 2 equiv of either arachidonate (1), EtOOH (2), 11,14-eicosadienoate (3), or 15-HPETE (5) at 15 °C in 50 mM potassium phosphate (pH 7.2) and 25% glycerol. In a separate experiment, indomethacin-treated (1 mol/mol of subunit) Mn–PGHS (3 μM subunit) was reacted with 2 equiv of 15-HPETE under the same conditions (4). Spectra were recorded with an HP Model 8452A diode array spectrophotometer, and the absorbance changes at 418 nm were corrected for base-line shifts by subtraction of the corresponding absorbance at one of the isosbestic points, 444 nm.

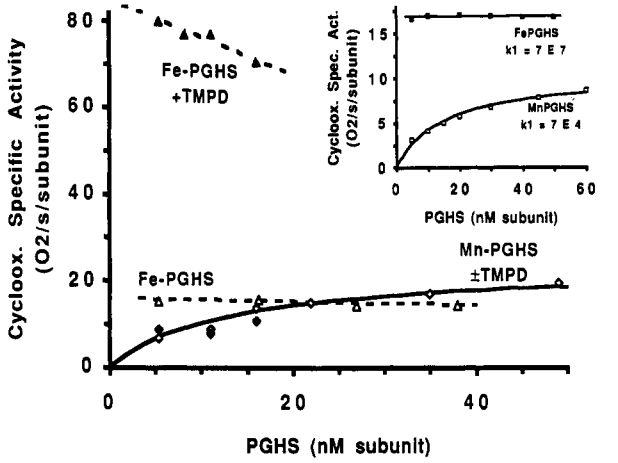

FIGURE 6: Effect of enzyme concentration on cyclooxygenase specific activity of Fe–PGHS and Mn–PGHS. PGHS was reconstituted with either Fe protoporphyrin IX (▲, △) or Mn protoporphyrin IX (●, ◇) and the indicated levels injected for assay of the cyclooxygenase activity in the presence (▲, ●) or absence (△, ◇) of 84 μM TMPD in cuvettes containing 3 mL of 0.1 M potassium phosphate (pH 7.2) and 100 μM arachidonate at 30 °C. The cyclooxygenase specific activity was obtained by dividing the cyclooxygenase V_{opt} by the synthase concentration. Inset: Predicted dependence of cyclooxygenase specific activity on the enzyme level. Cyclooxygenase reaction kinetics were simulated by numerical integration of a set of differential equations based on the reaction mechanism in Scheme 1 (Kulmacz et al., 1994). The values of individual rate constants were as follows: k_1, 7×10^7 or 7×10^4 M^{-1} s^{-1}; k_2, 1.5×10^7 M^{-1} s^{-1}; k_3, 1.5×10^6 M^{-1} s^{-1}; k_4, 1.75×10^3 s^{-1}; k_5 (a lumped constant encompassing the k_5, k_7, and k_8 cyclooxygenase steps), 90 s^{-1}; k_6, 0.07 s^{-1}; k_6', 0.38 s^{-1}; and k_9, 22 M^{-1} s^{-1}. These parameter values are for reaction at 30 °C, the temperature for the standard cyclooxygenase assay, and were found to provide satisfactory simulation of the cyclooxygenase reaction kinetics of Fe–PGHS under a wide variety of conditions.

Scheme 1: Hypothetical Reaction Mechanism for Fe–PGHS[a]

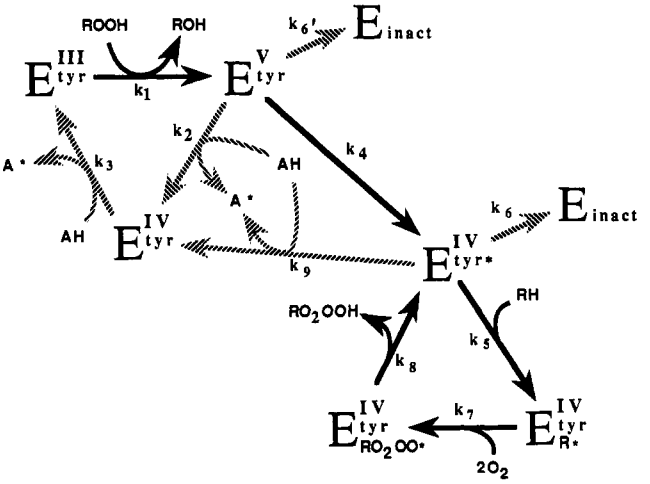

[a] Adapted from the proposal by Karthein et al. (1988). The roman numerals indicate the formal oxidation state of the heme iron; tyr and tyr* represent a tyrosine residue and the corresponding tyrosyl radical; RH, R*, RO_2O*, and RO_2OOH represent arachidonate, an arachidonyl radical, the peroxy radical of PGG_2, and PGG_2, respectively; ROOH and ROH represent hydroperoxide and the corresponding alcohol; AH and A* represent reduced and oxidized cosubstrate; and E_{inact} represents self-inactivated enzyme. Hatched (gray) arrows are used for dissipative processes to focus attention on the initiation and propagation of cyclooxygenase catalysis.

cyclooxygenase activity was not a linear function of the level of added Mn–PGHS (data not shown). To investigate this further, the effects of enzyme concentration on the cyclooxygenase specific activities of Mn–PGHS and Fe–PGHS were examined with and without TMPD present. With Fe–PGHS in the absence of TMPD, the cyclooxygenase specific activity was relatively independent of the enzyme concentration in the range of 5.4–38 nM subunit (Figure 6). When assayed in the presence of the reducing cosubstrate TMPD, the cyclooxygenase specific activity of Fe–PGHS was increased about 5-fold and declined somewhat as the enzyme concentration was increased.

With Mn–PGHS in the absence of TMPD, the specific activity increased 3-fold when the enzyme concentration was raised from 5 to 49 nM subunit (Figure 6); this increase can be fit to the Michaelis–Menten formula. The estimated maximal specific activity was 23.5 mol of O_2/s/mol of subunit, with half-saturation reached at 13.3 nM Mn–PGHS. Thus, in the absence of cosubstrate, Mn–PGHS was capable of producing fatty acid hydroperoxide at a somewhat faster rate than that seen with Fe–PGHS. Whereas the presence of 84 μM TMPD had little or no effect on the cyclooxygenase specific activity of Mn–PGHS (Figure 6), the extent of oxygen consumption by Mn–PGHS before self-inactivation was increased by more than 2-fold in the presence of TMPD (data not shown).

The increase in Mn–PGHS cyclooxygenase specific activity with enzyme level was surprising, and its cause was not intuitively obvious. The possibility that it was related to the very much slower rate of reaction of the Mn–PGHS peroxidase with hydroperoxide (see above) was tested using a computational model for the simulation of cyclooxygenase reaction kinetics based on the mechanism in Scheme 1 (Kulmacz et al., 1994). The cyclooxygenase reaction kinetics were first simulated for several enzyme concentrations (5–50 nM subunit) in the absence of cosubstrate using the parameter set for Fe–PGHS. Then, another set of simulations was run with the value of the rate constant for the reaction of peroxidase with hydroperoxide (k_1 in the mechanism in Scheme 1) decreased from 7×10^7 to 7×10^4 M^{-1} s^{-1}. The cyclooxygenase specific activities calculated from these simulations are shown in the inset to Figure 6. With the lower value of k_1 appropriate for Mn–PGHS, the cyclooxygenase specific activity is pre-

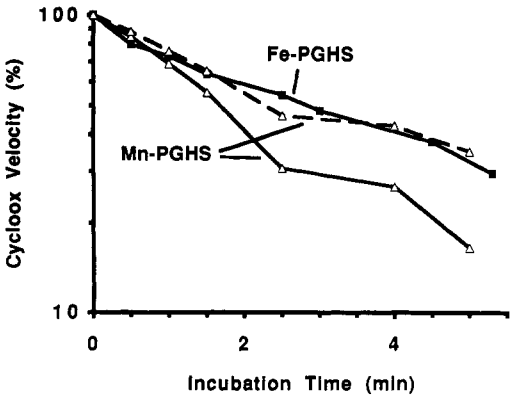

FIGURE 7: Inhibition of the cyclooxygenase activity of Mn–PGHS and Fe–PGHS by TNM. Mn–PGHS and Fe–PGHS were incubated separately at 23 °C with 0.5 mM TNM in 0.1 M Tris (pH 8.0). After the indicated times, fixed aliquots (96 pmol of subunit for Mn–PGHS and 87 pmol of subunit for Fe–PGHS) were injected into the standard cyclooxygenase assay system supplemented with MnPPIX or FePPIX (1 μM). Surviving activities are presented as the percentage of the initial value (112 nmol of O_2/min for Mn–PGHS and 288 nmol of O_2/min for Fe–PGHS). The upper set of points for Mn–PGHS (– –) represent the values corrected for inefficient initiation, as described in the text.

dicted to increase with enzyme concentration over the range used experimentally. In contrast, with the higher value of k_1 appropriate for Fe–PGHS, the cyclooxygenase specific activity is predicted to be insensitive to the enzyme level.

Inhibition of the Cyclooxygenase Activity of Mn–PGHS by TNM. The ability of TNM, a reagent that selectively nitrates tyrosyl residues (Sokolovsky et al., 1966), to inhibit the cyclooxygenase activity in Mn–PGHS was examined. The cyclooxygenase velocity in Mn–PGHS was destroyed in an exponential fashion with an apparent rate constant of 0.38 min^{-1}, which is somewhat higher than the value of 0.25 min^{-1} obtained with Fe–PGHS (Figure 7). Because the observed cyclooxygenase specific activity of Mn–PGHS increases with the absolute amount of activity expressed (Figure 6), the activities observed at later times in the incubation with TNM underestimate the actual activity surviving. To correct for this, a calibration curve for the fraction of maximal specific activity versus observed activity was constructed from the Mn–PGHS data in Figure 6. This calibration curve was used to estimate the actual surviving activity in TNM-treated Mn–PGHS. Once corrected, the data for the destruction of cyclooxygenase activity by TNM in Mn–PGHS were almost superimposable on those for Fe–PGHS (Figure 7). This makes it likely that cyclooxygenase inactivation in Mn–PGHS and Fe–PGHS results from modification of the same essential tyrosine residue(s).

Generation of Free Radicals during the Reaction of Mn–PGHS with Substrates. Reaction of Mn–PGHS with 2 equiv of arachidonate was able to produce rapidly a free radical EPR signal with a peak-to-trough width of about 38 G (Figure 8, spectrum A), which is somewhat larger than the wide singlet observed in later stages of the reaction of Fe–PGHS with low levels of the fatty acid (Tsai et al., 1992). Reaction of Mn–PGHS with 2 equiv of 15-HPETE yielded a similar radical EPR signal (Figure 8, spectrum B). No significant radical species were detected in reactions of Mn–PGHS with EtOOH (not shown). Addition of 2 equiv of 15-HPETE to Mn–PGHS that had been pretreated with TNM to inactivate the cyclooxygenase activity resulted in a markedly narrower EPR singlet, with a peak-to-trough width of only 19 G (Figure 8, spectrum C). This signal is considerably narrower than that in TNM-treated Fe–PGHS (26 G peak-to-trough; Kulmacz et al., 1990). The radical species from reactions of Mn–PGHS and TNM-treated Mn–PGHS with 15-HPETE and of Mn–PGHS with arachidonate all had $P_{1/2}$ values around 3 mW at liquid nitrogen temperature, indicating similar interactions with the paramagnetic MnPPIX center.

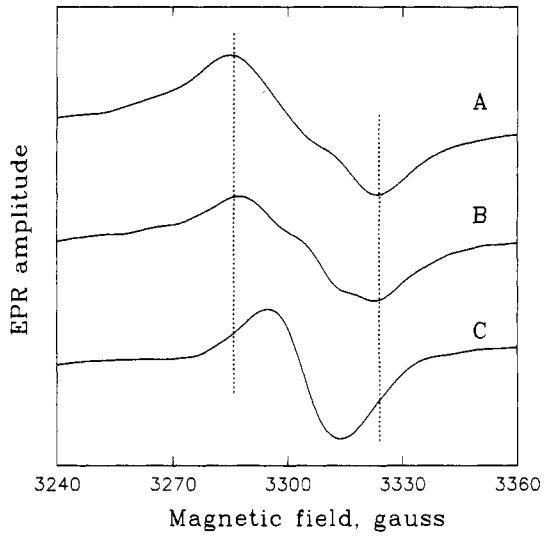

FIGURE 8: EPR spectra in the $g = 2$ region of Mn–PGHS substrate-induced radicals. Mn–PGHS (21 μM subunit in 50 mM potassium phosphate (pH 7.2), 30% glycerol, and 0.02% octyl glucoside) was reacted at 0 °C with 2 equiv of arachidonate for 9 s (spectrum A) or 2 equiv of 15-HPETE for 7 s (spectrum B). Spectrum C: Mn–PGHS was pretreated with 1 mM TNM at room temperature until 5% of the cyclooxygenase activity remained. Excess reagent was removed by gel filtration, and the TNM-treated enzyme (17 μM subunit) was then reacted with 2 equiv of 15-HPETE for 8 s at 0 °C. EPR spectra were obtained at 93 K with instrument settings as follows: power, 1 mM; modulation amplitude, 8 G; frequency, 9.22 MHz. Eight scans were averaged for each spectrum.

The intensities of the radicals induced by 15-HPETE in Mn–PGHS, TNM-treated Mn–PGHS, indomethacin-treated Mn–PGHS, and PGHS apoenzyme were examined as a function of incubation time. These results are shown in Figure 9, along with those for control Mn–PGHS. No significant radical intensity was observed with control Mn–PGHS or indomethacin-treated Mn–PGHS reacted with 15-HPETE. Double integration indicated that PGHS apoenzyme reacted with 15-HPETE did produce a very small amount of radical (0.015 spin/subunit), although the shape of the signal was not discernible because of the noise in the original spectrum (data not shown). The radical intensity in Mn–PGHS reacted with 15-HPETE was maximal (0.062 spin/subunit) at the first time point examined (7 s) and then gradually declined. The radical induced by 15-HPETE in TNM-treated Mn–PGHS accumulated slightly more slowly, peaking at 0.051 spin/subunit after 50 s and then declining. The line shape of the radicals in Mn–PGHS and TNM-treated Mn–PGHS did not change perceptibly as a function of time.

Kinetics of Radical Accumulation during the Reaction of Mn–PGHS with Arachidonate. A distinct EPR radical signal was apparent after 1 s of reaction of Mn–PGHS with 2 equiv of arachidonate (Figure 10). This radical was an isotropic singlet with an approximately 36–38 G peak-to-trough width, which is somewhat wider than the doublet and singlet observed during the reaction of Fe–PGHS with stoichiometric arachidonate (32–34 G peak-to-trough; Tsai et al., 1992). The 36–38 G singlet was centered at $g = 2.005$ and had a similar line shape at both liquid nitrogen and liquid helium temperatures (not shown). The intensity of the signal in Mn–PGHS increased over the next few seconds, reaching an initial plateau

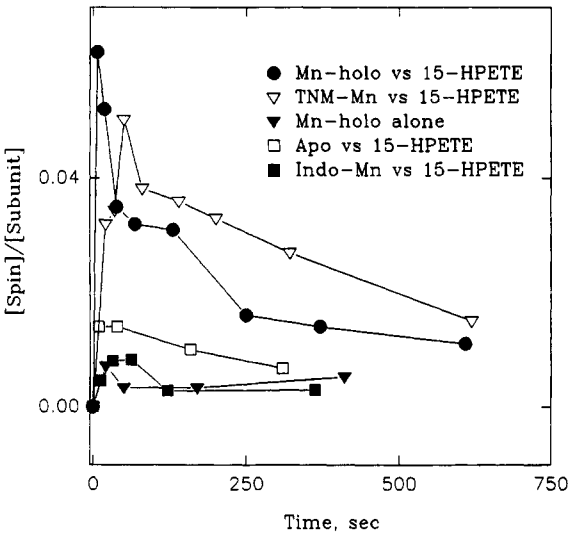

FIGURE 9: Kinetics of accumulation of radicals induced by 15-HPETE. For the initial time point, 2 equiv of 15-HPETE were incubated with PGHS apoenzyme (20 μM subunit), Mn–PGHS (21 μM subunit), TNM-treated (see legend to Figure 8) Mn–PGHS (17 μM subunit), or indomethacin-treated (1 mol/mol of subunit) Mn–PGHS (21 μM subunit) for 7–20 s at 0 °C before the reaction was quenched by freezing in dry ice/acetone. The initial EPR spectra were then recorded at liquid nitrogen temperature, and the intensity of the signal in the $g = 2$ region was estimated by double integration (Materials and Methods). Longer incubations were obtained by thawing samples at 0 °C for the desired time increments and then refreezing the samples and recording their EPR spectra (Kulmacz et al., 1990). 15-HPETE was omitted from the Mn–PGHS control.

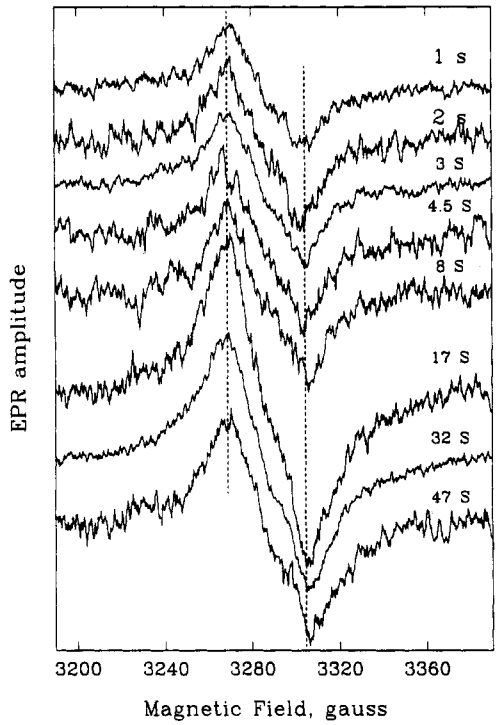

FIGURE 10: EPR spectra in the $g = 2$ region during Mn–PGHS reaction with arachidonate. Equal volumes of Mn–PGHS (30 μM subunit) and arachidonate (60 μM) were mixed at 0 °C using a two-syringe device and incubated for the indicated times (Materials and Methods). EPR spectra were obtained at 98 K with instrument settings as follows: power, 1 mM; modulation amplitude, 2 G; frequency, 9.22 MHz. The amplitudes of individual spectra are corrected for differences in EPR sample tube diameter.

of 0.05 spin/subunit at 5–8 s and then increasing again to 0.13 spin/subunit at 17 s before declining slowly (Figure 11). No gross change was seen in the line shape of the singlet

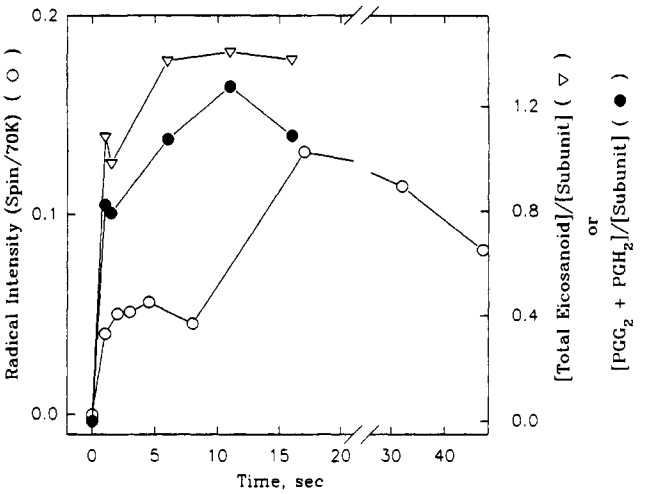

FIGURE 11: Kinetics of arachidonate metabolism and radical intensity during reaction of Mn–PGHS with arachidonic acid. Mn–PGHS was reacted with 2 equiv of arachidonate, as described in the legend to Figure 9. Conversion of arachidonate to PGG_2 and PGH_2 (●) or total eicosanoids (△) was determined by chromatographic analysis of radiolabeled products. The intensity of the wide singlet radical signal (○) was obtained from double integration of the EPR signals shown in Figure 9, with reference to a copper sulfate standard.

during the reaction, suggesting that the same radical species was present throughout. Subtle changes in the spectra might, however, be obscured by the noise. The radical intensity was considerably greater than could be accounted for by the small amount of residual functional FePPIX in the sample (see Figure 9 and Table 1), confirming that the signal originated from Mn–PGHS and not from Fe–PGHS.

Cyclooxygenase activity was monitored by chromatographic quantitation of PGG_2 and PGH_2 during the reaction of Mn–PGHS with arachidonate under the same conditions used for the EPR study just described, using the same batch of Mn–PGHS. The reaction was very rapid, with significant prostaglandin synthesized after 1–2 s of incubation (Figure 11). The increases in total eicosanoids paralleled those in PGG_2 and PGH_2, confirming that arachidonate was being converted to the expected cyclooxygenase products. Cyclooxygenase activity thus coincided with the initial appearance of the 36–38 G free radical. The cyclooxygenase reaction was complete by 11 s, when essentially no arachidonate remained. Depletion of substrate fatty acid thus coincided with the secondary accumulation of radical intensity (Figure 11).

DISCUSSION

Prosthetic Group Substitution and Peroxidase Characteristics. Substitution of MnPPIX for FePPIX had dramatic effects on the peroxidase activity, as would be expected from the central role of the metalloporphyrin in the catalytic mechanism. The steady-state turnover with lipid hydroperoxides was about 26-fold lower for Mn–PGHS than for Fe–PGHS (see Results). The rate constant for formation of the oxidized Mn–PGHS peroxidase intermediate upon reaction with 15-HPETE can be roughly estimated to be on the order of 10^4 M^{-1} s^{-1} from the data in Figure 5. This is comparable to the value of 4×10^4 M^{-1} s^{-1} reported by Strieder et al. (1992) for the reaction of Mn–PGHS with 5-phenyl-4-pentenyl hydroperoxide, but about 3 orders of magnitude slower than the rate constant for compound I formation during the reaction of Fe–PGHS with lipid hydroperoxides (Lambeir et al., 1985; Kulmacz, 1986; Dietz et al., 1988; MacDonald et al., 1989).

The large difference in peroxidase substrate specificity between Mn–PGHS and Fe–PGHS, with the affinity for lipid hydroperoxides little changed but the affinity for water-soluble hydroperoxides much decreased in Mn–PGHS (see Results), suggests that the metalloporphyrin is a major part of the binding site for water-soluble hydroperoxides but has a smaller influence on the binding of physiological lipid hydroperoxides. As a consequence of the enhanced selectivity of the Mn–PGHS peroxidase for lipid substrates, the use of the small, water-soluble substrates such as HOOH, EtOOH, and 5-phenyl-4-pentenyl hydroperoxide is likely to result in significant underestimation of the peroxidase activity. This may explain the considerably lower estimates of peroxidase activity in Mn–PGHS in earlier reports (Ogino et al., 1978; Thompson & Eling, 1989; Odenwaller et al., 1992; Strieder et al., 1992). The disproportionately slower reactions of the small hydroperoxides with Mn–PGHS may also explain their inability to generate significant amounts of free radical, in contrast to the actions of lipid hydroperoxides (see Results; Lassmann et al., 1991; Strieder et al., 1992).

The striking differences in the stoichiometry of cosubstrate oxidation and in reaction products between Mn–PGHS and Fe–PGHS (Figures 1–4 and Table 2) demonstrate that the transfer of reducing equivalents to oxidized peroxidase intermediates is fundamentally altered by the change in prosthetic group. Formation of keto diene, as well as of hydroxy fatty acid, is a clear indication that the lipid substrate can act as both reductant and oxidant during peroxidase catalysis by Mn–PGHS. The observed generation of roughly equal amounts of 15-HETE and keto diene (Figure 2), with a TMPD oxidation stoichiometry of about 1 (Table 2), during the reaction of Mn–PGHS with 15-HPETE can be accounted for by the sum of equal amounts of two reactions:

reaction 1 $$\text{15-HPETE} + 2\ \text{TMPD} + 2\text{H}^+ \rightarrow \text{15-HETE} + 2\ \text{TMPDox} + \text{HOH}$$

reaction 2 $$\text{15-HPETE} + 2\text{H}^+ \rightarrow \text{15-KETE} + \text{HOH}$$

sum $$2\ \text{15-HPETE} + 2\ \text{TMPD} + 4\text{H}^+ \rightarrow \text{15-HETE} + \text{15-KETE} + 2\ \text{TMPDox} + 2\text{HOH}$$

Reaction 1 is the conventional peroxidase reaction: 15-HPETE is converted to 15-HETE, oxidizing the enzyme by 2 equiv; 15-HETE then dissociates, and 2 equiv of TMPD are oxidized to reduce the enzyme back to the resting state. In reaction 2, 15-HPETE is converted to 15-HETE, oxidizing the enzyme by 2 equiv. The resulting 15-HETE is then oxidized by 2 equiv to the keto diene (15-KETE), regenerating the resting enzyme. It should be noted that Mn–PGHS is assumed to be initially oxidized by 2 equiv in both reactions. A two-electron oxidation of Mn–PGHS is supported by the observations that the corresponding alcohols can be formed from 15-HPETE (Figure 2) and 5-phenyl-4-pentenyl hydroperoxide (Odenwaller et al., 1992) and that the stoichiometry of TMPD oxidation does approach 2 with PGG_2 (Table 2). It is not yet certain whether the single optical intermediate that accumulates during the peroxidase reaction is a Mn^V or a Mn^{IV} species (Odenwaller et al., 1992; Strieder et al., 1992).

Reaction of Mn–PGHS with 20:2, which presumably produces 11-HPEDE (Hemler et al., 1978a), resulted in the oxidation of about 1 equiv of TMPD (Table 2) and the formation of a lipid keto diene chromophore (Figure 4). Odenwaller et al. (1992) also reported an increase in absorbance at 286 nm during the reaction of Mn–PGHS with 20:2, which is consistent with the spectrum of a keto diene fatty acid in neutral buffer. Thus, both substrates which gave an unexpectedly low stoichiometry of TMPD oxidation with Mn–PGHS (Table 2) produced compounds with a keto diene absorbance spectrum, compounds that were essentially absent from the corresponding reactions with Fe–PGHS (Figures 3 and 4). This correlation further supports the concept that two alternative peroxidase reaction pathways (reactions 1 and 2) are available to Mn–PGHS, but only one (reaction 1) is available to Fe–PGHS. The biochemical basis for the formation of keto diene by Mn–PGHS but not by Fe–PGHS is unclear. The initial peroxidase intermediate in Mn–PGHS may be a stronger or better positioned oxidant than the corresponding intermediate in Fe–PGHS. In this regard, model studies with manganioporphyrins have found the Mn^{IV} state to be a very strong oxidant (Loach & Calvin, 1963), suggesting that the Mn^V state of MnPPIX in the synthase could be an extraordinarily powerful oxidant. Alternatively, the hydroxy fatty acid may dissociate significantly more slowly from the oxidized intermediate in Mn–PGHS than in Fe–PGHS, making oxidation of the lipid more likely.

Because reaction 1 requires TMPD and reaction 2 does not, it might be expected that increasing the level of TMPD would selectively increase the rate of reaction 1 and, thus, increase the stoichiometry of TMPD oxidation. This effect indeed was observed for TMPD levels between 10 and 84 μM, but further increases in the TMPD level did not increase the stoichiometry above about 1 with Mn–PGHS (Figure 1). This upper limit suggests that 15-HETE was used as the preferred cosubstrate by Mn–PGHS about half the time, even in the presence of saturating levels of TMPD. Further experimentation will be required to determine whether this apparent dichotomy in the fate of 15-HETE with Mn–PGHS reflects some heterogeneity in MnPPIX or substrate binding or reflects the relative probabilities of two paths at a critical juncture of the reaction process.

The observation of a significantly higher TMPD oxidation stoichiometry for Mn–PGHS with PGG_2 than with 15-HPETE or 11-HPEDE (Table 2) suggests that PGH_2 is not as efficient an electron donor as 15-HETE or 11-HEDE in reaction 2. This may be because oxidation of the C-15 alcohol of PGH_2 results in a ketone conjugated to an isolated double bond, whereas oxidation of the corresponding alcohols in 15-HETE or 11-HEDE produces lower energy conjugated keto dienes.

The influence of hydroperoxide structure can also be seen in the relaxation rates of oxidized Mn–PGHS intermediate (Figure 5). Reduction of the oxidized intermediate was rapid in reactions with 15-HPETE and 11,14-eicosadienoic acid and slow in reaction with arachidonate. Thus, the hydroperoxide substrates that produced faster decay of the oxidized Mn–PGHS intermediates were those that were able to serve as alternate reductants, suggesting that lipids were directly reducing the enzyme intermediates. The rate of the decay of the oxidized intermediate was independent of the concentration of 15-HPETE over the range of 20–400 μM (C. Wei and A.-L. Tsai, unpublished observations). This rules out 15-HPETE itself as the reductant and suggests that the electrons were furnished instead by newly formed 15-HETE before it dissociated from the oxidized enzyme. The very slow relaxation of oxidized intermediate during the reaction with EtOOH (Figure 5) is consistent with the inability of this substrate to furnish reducing equivalents.

Some alternative explanations for the low stoichiometry of TMPD oxidation with Mn–PGHS appear unlikely because they do not account for all observations. A single reaction in

which one reducing equivalent is furnished by bound 15-HETE and the other by TMPD is consistent with the observed TMPD oxidation stoichiometry, but should result in a single lipid product, not the two observed. Lipid hydroperoxides themselves are known to act as reductants with soybean lipoxygenase under anaerobic conditions, but this process requires unoxidized fatty acid and produces shorter chain scission products, as well as a keto diene (Garssen et al., 1971). Such scission products would be more polar than 15-HETE; no such products were observed (Figure 2).

The inhibition of Mn–PGHS peroxidase activity by the anti-cyclooxygenase agent, indomethacin, evident from the decreased level of oxidized intermediate (Figure 5) and the lower steady-state velocity (see Results), is in contrast to this agent's lack of an effect on the Fe–PGHS peroxidase activity (Mizuno et al., 1982). There is one report that indomethacin partially inhibits the reduction of oxidized Fe–PGHS intermediates by cosubstrates such as phenol (Hsuanyu & Dunford, 1992). However, this effect required much higher levels of indomethacin (EC_{50} ca. 30 μM) than those used here with Mn–PGHS (0.1 μM for steady-state assays and 3 μM for the observation of oxidized intermediate). In contrast with indomethacin-treated Fe–PGHS (Kulmacz et al., 1990), no significant radical signal was detected when 15-HPETE was added to indomethacin-treated Mn–PGHS (Figure 9). This inability to accumulate significant radical in indomethacin-treated Mn–PGHS is consistent with the low levels of oxidized intermediate produced by 15-HPETE (Figure 5). It appears that indomethacin interferes with the initial interaction between Mn–PGHS and hydroperoxide because accumulation of the oxidized intermediate was dramatically decreased (Figure 5), whereas the rate of oxidation of cosubstrate in the steady-state assay was inhibited by only one-third (see Results).

Prosthetic Group Substitution and Cyclooxygenase Characteristics. The cyclooxygenase specific activity of Mn–PGHS increased with the amount of enzyme assayed; this behavior clearly is different from that seen with Fe–PGHS (Figure 6). This contrasting behavior was surprising, but the mechanism in Scheme 1 predicts just such a difference (inset to Figure 6) when the value of a single rate constant, that governing the rate of formation of oxidized peroxidase intermediate (k_1 in Scheme 1), is decreased in keeping with experimental observations (see Results; Strieder et al., 1992). The ability of the mechanism in Scheme 1 to account for an unanticipated change in cyclooxygenase reaction kinetics based on a simple change in peroxidase kinetics further supports the proposed mechanistic linkage between the two activities and demonstrates the usefulness of the mechanistic model in interpreting the complex behavior of the synthase. The cyclooxygenase specific activity of Fe–PGHS is also likely to be dependent on the enzyme level, but at activities below those easily assayed with the oxygen electrode. In this respect, the change in prosthetic group made this aspect of the cyclooxygenase reaction more amenable to direct observation. Even with Mn–PGHS, the dependence of cyclooxygenase specific activity on the enzyme level was apparent only below 50 nM enzyme (Figure 6) and, thus, would not be noticed at the 1–1.5 μM levels used in recent studies (Odenwaller et al., 1992; Strieder et al., 1992).

An increased sensitivity to suppression by glutathione peroxidase has shown that Mn–PGHS requires a considerably higher level of hydroperoxide to sustain effective initiation of the cyclooxygenase activity (K_p value of 100 nM PGG_2, compared to 20 nM for Fe–PGHS; Kulmacz, 1991); similar results have been reported by other workers (Odenwaller et al., 1992; Strieder et al., 1992). In the absence of a reducing cosubstrate, the maximal rate of fatty acid hydroperoxide formation with Mn–PGHS was somewhat higher than that with Fe–PGHS (Figure 6), indicating that MnPPIX did not impair steps involved in propagation of the cyclooxygenase reaction. This impairment of cyclooxygenase initiation but not cyclooxygenase propagation upon substitution of MnPPIX for FePPIX supports the concept that the metalloporphyrin has a direct role in cyclooxygenase initiation, but an indirect role in cyclooxygenase propagation, as is implicit in the mechanism in Scheme 1.

The more than 2-fold increase in the extent of the Mn–PGHS cyclooxygenase reaction before self-inactivation upon the addition of TMPD (see Results) demonstrates that Mn–PGHS cyclooxygenase was sensitive to the presence of reducing cosubstrates, even though TMPD had no effect on the cyclooxygenase velocity (Figure 6). Strieder et al. (1992) reported that the addition of diethyl dithiocarbamate prevented stimulation of the Mn–PGHS cyclooxygenase velocity by phenol. This would be consistent with our results, because diethyl dithiocarbamate is used in our enzyme purification. With Fe–PGHS, reducing cosubstrates produce parallel increases in cyclooxygenase velocity and extent (Kulmacz & Lands, 1985a). It is interesting to note that millimolar levels of cyanide blocked the stimulatory effect of phenol on the Fe–PGHS cyclooxygenase velocity, but not the stimulatory effect on reaction extent; cyanide also inhibited the peroxidase activity and increased the hydroperoxide requirement for cyclooxygenase initiation (Kulmacz & Lands, 1985a). These parallels between the kinetic effects of heme liganding by cyanide and heme substitution by MnPPIX confirm that these effects are due to an alteration of the prosthetic group function rather than to some nonspecific structural perturbations in the protein.

Prosthetic Group Substitution and PGHS Free Radical Characteristics. Lipid hydroperoxides, either added directly or generated in situ from arachidonate, are able to generate free radicals in Mn–PGHS (Figure 8). The peak intensity of the Mn–PGHS radical species in reactions with 15-HPETE (0.06 spin/subunit; Figure 9) was about one-third that observed with Fe–PGHS (0.19 spin/subunit; Kulmacz et al., 1990). This lower accumulation of radical in Mn–PGHS is consistent with the postulated radical formation from oxidized peroxidase intermediates, intermediates that form more slowly in Mn–PGHS than in Fe–PGHS (see Results; Odenwaller et al., 1992; Strieder et al., 1992). The selectivity of Mn–PGHS peroxidase for lipid hydroperoxides (see Results; Figure 5) may explain the difficulty in generating a detectable radical signal in reactions of Mn–PGHS with EtOOH (see Results) or with PPHP (Lassmann et al., 1991; Strieder et al., 1992).

The wide singlet EPR signal observed upon mixing Mn–PGHS with either arachidonate or 15-HPETE, with a peak-to-trough width of about 36–38 G (Figure 8, spectra A and B), is wider than either the wide doublet or the wide singlet tyrosyl radicals observed in similar Fe–PGHS reactions (about 32–34 G peak-to-trough; Karthein et al., 1988; Tsai et al., 1992). However, the $P_{1/2}$ of the Mn–PGHS singlet, about 3 mW at liquid nitrogen temperatures (see Results), was comparable to that of the Fe–PGHS doublet (5–6 mW; Tsai et al., 1992). The power saturation behavior of the radicals in both Fe–PGHS and Mn–PGHS suggests that the radicals are near the metalloporphyrin.

From the proposed reaction mechanism for cyclooxygenase activity (Scheme 1), it is expected that a tyrosyl radical should be present during cyclooxygenase activity. The wide doublet

tyrosyl radical (34 G peak-to-trough) was detected early in the reaction of Fe–PGHS with equimolar arachidonate, and its intensity increased somewhat after the fatty acid was exhausted (Tsai et al., 1992). A free radical was also detected soon after mixing arachidonate with Mn–PGHS under similar conditions, and this radical also accumulated further after the fatty acid substrate was used up (Figures 10 and 11). In both Mn–PGHS and Fe–PGHS the radical was detectable during cyclooxygenase catalysis. Accumulation of radical after exhaustion of the fatty acid is exactly the behavior expected for a catalytic intermediate that continues to be formed (the hydroperoxide PGG_2 is still present) but cannot be utilized (the substrate fatty acid is depleted). The intensity of the 36–38 G singlet in Mn–PGHS during cyclooxygenase activity in the first few seconds of incubation with arachidonate (0.05 spin/subunit; Figure 11) was essentially the same as that of the Fe–PGHS wide tyrosyl radical doublet (Tsai et al., 1992). The fraction of synthase protein actually in cyclooxygenase catalytic cycle intermediates at the time of maximum cyclooxygenase velocity can be roughly estimated at 0.2 (Tsai et al., 1992). Considering that any protein radical species would be only one of several enzyme intermediates in the cyclooxygenase cycle, the peak concentration of the protein radical intermediate would be expected to be some fraction of 0.2 spin/subunit. Thus, the 36–38 G singlet appeared at the appropriate time, and in an appropriate amount, for a catalytically competent intermediate in the Mn–PGHS cyclooxygenase reaction.

Nitration of only about 3 of the 27 tyrosine residues accompanied Fe–PGHS cyclooxygenase inactivation by TNM (Kulmacz et al., 1990; Shimokawa et al., 1990). TNM inactivated Mn–PGHS at essentially the same rate as Fe–PGHS (Figure 7), indicating that cyclooxygenase catalyses by Mn–PGHS and Fe–PGHS share a requirement for the same TNM-sensitive tyrosine residue(s). Just as was observed with Fe–PGHS, the inactivation of Mn–PGHS by TNM resulted in a marked narrowing of the hydroperoxide-induced radical signal (Figure 8; Kulmacz et al., 1990), indicating that tyrosine residues influence the radical structure in Mn–PGHS. Despite these parallels, the spectra of the radicals in Mn–PGHS and TNM-treated Mn–PGHS are quite distinct from the corresponding spectra for the tyrosyl radicals in Fe–PGHS (Figure 8; Kulmacz et al., 1990; DeGray et al., 1992). Other radical species, including glycine radicals, have been reported to have EPR spectra roughly similar to those of the tyrosyl radicals (Sivarajah et al., 1989; Wagner et al., 1992; Nelson et al., 1993). It is thus unclear whether the Mn–PGHS radicals are actually tyrosyl radicals. A definitive test of this issue will require the preparation of Mn–PGHS with deuterated tyrosyl residues, as was done for Fe–PGHS (Tsai et al., 1994) and for ribonucleotide reductase (Graslund et al., 1982).

Lassmann et al. (1991) have examined the EPR of Mn–PGHS during reaction with excess arachidonate and found that a very narrow and weak singlet (16 G peak-to-trough) was present after 1–2 min of reaction, with a wider (36 G peak-to-trough) singlet prevailing after 3 min of reaction. The bulk of product formation was complete at the first time point examined, 1 min, with only about 1 mol of eicosanoids formed/mol of synthase, and a significant accumulation of radical was not observed until after oxygenase activity had ceased. Thus, the reaction conditions used by Lassmann et al. (1991) led to abnormally efficient self-inactivation for Mn–PGHS. As a consequence, cyclooxygenase turnover and complete self-inactivation of the enzyme were occurring simultaneously during the first minute of the incubation; this makes it difficult to observe any EPR signals associated with the rapidly diminishing fraction of catalytically competent enzyme. The present examination of the kinetics of radical formation during cyclooxygenase catalysis by Mn–PGHS (Figures 10 and 11) used only 2 equiv of arachidonate/active center; this low molar ratio has been found to minimize the extent of self-inactivation (Tsai et al., 1992). The Mn–PGHS radical thus observed in our studies can reasonably be attributed to normal cyclooxygenase catalysis.

Reaction Mechanism of Mn–PGHS. Mn–PGHS possesses two essential elements of the mechanism proposed for Fe–PGHS (Scheme 1): (i) reaction with hydroperoxides to generate an oxidized enzyme intermediate and (ii) formation of a free radical coincident with cyclooxygenase catalysis. As mentioned previously, $Mn^{V}PPIX$ and $Mn^{IV}PPIX$ are likely to be very strong oxidants (Loach & Calvin, 1963). The hydroperoxide reaction product of Mn–PGHS with MnPPIX in either the IV or V state should thus be able to oxidize a tyrosine residue (or an alternative residue) to form the radical needed for cyclooxygenase catalysis, as is proposed to occur with Fe–PGHS (Scheme 1).

As with Fe–PGHS, the cyclooxygenase activity of Mn–PGHS has feedback activation by PGG_2, as demonstrated by the stimulatory effect of added hydroperoxide (Hemler et al., 1978b) and by the inhibitory effect of hydroperoxide scavenger (Kulmacz, 1991; Strieder et al., 1992; Odenwaller et al., 1992). This feedback activation by PGG_2 is consistent with the proposed role of hydroperoxide in the initiation of the cyclooxygenase reaction (Scheme 1). Further, Mn–PGHS reacts much more slowly with hydroperoxides than does Fe–PGHS and, as a consequence, would be expected to be less efficient in cyclooxygenase initiation. The higher hydroperoxide requirement for Mn–PGHS ($K_p \sim 100$ nM PGG_2) than for Fe–PGHS ($K_p \sim 20$ nM) determined by a competition method (Kulmacz, 1991) qualitatively bears out this expectation. However, the 5-fold difference between Mn–PGHS and Fe–PGHS in the hydroperoxide initiator requirement is much less than the 1000-fold difference in the rate of reaction with hydroperoxide to form oxidized intermediates (see Results; Streider et al., 1992). This suggests that formation of the oxidized peroxidase intermediate cannot be the rate-determining step for initiation in both Fe–PGHS and Mn–PGHS.

Overall, the kinetic characteristics of Mn–PGHS are quite consistent with the general features of the reaction mechanism proposed for Fe–PGHS. This mechanism will thus provide a very useful framework for further investigation of the synthase and the many mutant forms produced by site-directed mutagenesis. In each case, the kinetic differences induced by the substitution of MnPPIX for heme may make it possible to characterize individual reaction steps that are not otherwise readily accessible.

ACKNOWLEDGMENT

We thank Mr. Jiong Deng for assistance in the purification of the synthase and Mr. Yong Ren for preliminary experiments with Mn–PGHS and TNM.

REFERENCES

DeGray, J. A., Lassmann, G., Curtis, J. F., Kennedy, T. A., Marnett, L. J., Eling, T. E., & Mason, R. P. (1992) *J. Biol. Chem. 267*, 23583–23588.

Dietz, R., Nastainczyk, W., & Ruf, H. H. (1988) *Eur. J. Biochem. 171*, 321–328.

Eling, T. E., Mason, R. P., & Sivarajah, K. (1985) *J. Biol. Chem. 260*, 1601–1607.
Garssen, G. J., Vliegenthart, J. F. G., & Boldingh, J. (1971) *Biochem. J. 122*, 327–332.
Graff, G. (1982) *Methods Enzymol. 86*, 386–392.
Graff, G., Anderson, L. A., & Jaques, L. W. (1990) *Anal. Biochem. 188*, 38–47.
Graslund, A., Ehrenberg, A., & Thelander, L. (1982) *J. Biol. Chem. 257*, 5711–5715.
Hemler, M. E., Crawford, C. G., & Lands, W. E. M. (1978a) *Biochemistry 17*, 1772–1779.
Hemler, M. E., Graff, G., & Lands, W. E. M. (1978b) *Biochem. Biophys. Res. Commun. 85*, 1325–1331.
Hsuanyu, Y. C., & Dunford, H. B. (1992) *Arch. Biochem. Biophys. 292*, 213–220.
Karthein, R., Dietz, R., Nastainczyk, W., & Ruf, H. H. (1988) *Eur. J. Biochem. 171*, 313–320.
Kulmacz, R. J. (1986) *Arch. Biochem. Biophys. 249*, 273–285.
Kulmacz, R. J. (1987) *Prostaglandins 34*, 225–240.
Kulmacz, R. J. (1991) in *Eicosanoids and Other Bioactive Lipids in Cancer and Radiation Injury* (Honn, K. V., Marnett, L. J., Nigam, S., & Walden, T., Jr., Eds.) pp 205–208, Kluwer Academic Publishers, Boston.
Kulmacz, R. J., & Lands, W. E. M. (1983) *Prostaglandins 25*, 531–540.
Kulmacz, R. J., & Lands, W. E. M. (1984) *J. Biol. Chem. 259*, 6358–6363.
Kulmacz, R. J., & Lands, W. E. M. (1985a) *Prostaglandins 29*, 175–190.
Kulmacz, R. J., & Lands, W. E. M. (1985b) *J. Biol. Chem. 260*, 12572–12578.
Kulmacz, R. J., & Lands, W. E. M. (1987) in *Prostaglandins and Related Substances: A Practical Approach* (Benedetto, C., McDonald-Gibson, R. G., Nigam, S., & Slater, T. F., Eds.) pp 209–227, IRL Press, Washington, D.C.
Kulmacz, R. J., Miller, J. F., Jr., & Lands, W. E. M. (1985) *Biochem. Biophys. Res. Commun. 130*, 918–923.
Kulmacz, R. J., Tsai, A.-L., & Palmer, G. (1987) *J. Biol. Chem. 262*, 10524–10531.
Kulmacz, R. J., Ren, Y., Tsai, A.-L., & Palmer, G. (1990) *Biochemistry 29*, 8760–8771.
Kulmacz, R. J., Palmer, G., & Tsai, A.-L. (1991) *Mol. Pharmacol. 40*, 833–837.
Kulmacz, R. J., Pendleton, R. B., & Lands, W. E. M. (1994) *J. Biol. Chem. 269*, 5527–5536.
Lambeir, A.-M., Markey, C. M., Dunford, H. B., & Marnett, L. J. (1985) *J. Biol. Chem. 260*, 14894–14896.
Lassmann, G., Odenwaller, R., Curtis, J. F., DeGray, J. A., Mason, R. P., Marnett, L. J., & Eling, T. E.. (1991) *J. Biol. Chem. 266*, 20045–20055.
Loach, P. A., & Calvin, M. (1963) *Biochemistry 2*, 361–371.
MacDonald, I. D., Graff, G., Anderson, L. A., & Dunford, H. B. (1989) *Arch. Biochem. Biophys. 272*, 194–202.
Marshall, P. J., Kulmacz, R. J., & Lands, W. E. M. (1987) *J. Biol. Chem. 262*, 3510–3517.
Miyamoto, T., Ogino, N., Yamamoto, S., & Hayaishi, O. (1976) *J. Biol. Chem. 251*, 2629–2636.
Mizuno, K., Yamamoto, S., & Lands, W. E. M. (1982) *Prostaglandins 23*, 743–757.
Nelson, M. J., Cowling, R. A., Seitz, S. P., Buck, C., & Scarrow, R. C. (1993) *FASEB J. 7*, A1059.
Odenwaller, R., Maddipati, K. R., & Marnett, L. J. (1992) *J. Biol. Chem. 267*, 13863–13869.
Ogino, N., Ohki, S., Yamamoto, S., & Hayaishi, O. (1978) *J. Biol. Chem. 253*, 5061–5068.
Peterson, G. L. (1983) *Methods Enzymol. 91*, 95–119.
Reed, G. A., Lasker, J. M., Eling, T. E., & Sivarajah, K. (1985) *Prostaglandins 30*, 153–165.
Shimokawa, T., Kulmacz, R. J., DeWitt, D. L., & Smith, W. L. (1990) *J. Biol. Chem. 265*, 20073–20076.
Sivaraja, M., Goodin, D. B., Smith, M., & Hoffman, B. M. (1989) *Science 245*, 738–740.
Sokolovsky, M., Riordan, J. F., & Vallee, B. L. (1966) *Biochemistry 5*, 3582–3589.
Strieder, S., Schaible, K., Scherer, H.-J., Dietz, R., & Ruf, H. H. (1992) *J. Biol. Chem. 267*, 13870–13878.
Thompson, D., & Eling, T. (1989) *Mol. Pharmacol. 36*, 809–817.
Tsai, A.-L., Palmer, G., & Kulmacz, R. J. (1992) *J. Biol. Chem. 267*, 17753–17759.
Tsai, A.-L., Hsi, L. C., Kulmacz, R. J., Palmer, G., & Smith, W. L. (1994) *J. Biol. Chem. 269*, 5058–5091.
Vioque, E., & Holman, R. T. (1962) *Arch. Biochem. Biophys. 99*, 522–528.
Wagner, A. F. V., Frey, M., Neugebauer, F. A., Schafer, W., & Knappe, J. (1992) *Proc. Natl. Acad. Sci. U.S.A. 89*, 996–1000.